Published online 24 October 2006 *Nucleic Acids Research, 2006, Vol. 34, No. 20* ***e138***
doi:10.1093/nar/gkl697

Paired termini stabilize antisense RNAs and enhance conditional gene silencing in *Escherichia coli*

Nobutaka Nakashima[1,2], Tomohiro Tamura[2,3] and Liam Good[1,*]

[1]Department of Cell and Molecular Biology, Programme for Genomics and Bioinformatics, Karolinska Institute, Berzelius väg 35, 171 77 Stockholm, Sweden, [2]Research Institute of Genome-based Biofactory, National Institute of Advanced Industrial Science and Technology (AIST), 2-17-2-1 Tsukisamu-Higashi, Toyohira-ku, 062-8517 Sapporo, Japan and [3]Laboratory of Molecular Environmental Microbiology, Graduate School of Agriculture, Hokkaido University, Kita-9, Nishi-9, Kita-ku, 060-8589 Sapporo, Japan

Received July 11, 2006; Revised August 21, 2006; Accepted September 8, 2006

ABSTRACT

Reliable methods for conditional gene silencing in bacteria have been elusive. To improve silencing by expressed antisense RNAs (asRNAs), we systematically altered several design parameters and targeted multiple reporter and essential genes in *Escherichia coli*. A paired termini (PT) design, where flanking inverted repeats create paired dsRNA termini, proved effective. PTasRNAs targeted against the *ackA* gene within the acetate kinase-phosphotransacetylase operon (*ackA-pta*) triggered target mRNA decay and a 78% reduction in AckA activity with high genetic penetrance. PTasRNAs are abundant and stable and function through an RNase III independent mechanism that requires a large stoichiometric excess of asRNA. Conditional *ackA* silencing reduced carbon flux to acetate and increased heterologous gene expression. The PT design also improved silencing of the essential *fabI* gene. Full anti-*fabI* PTasRNA induction prevented growth and partial induction sensitized cells to a FabI inhibitor. PTasRNAs have potential for functional genomics, antimicrobial discovery and metabolic flux control.

INTRODUCTION

Advanced genetics and metabolic engineering require reliable conditional gene control. Unfortunately, gene disruption techniques remain difficult, applicable to a restricted set of species and strains and are particularly problematic in cases where the target gene is growth critical. In many eukaryotic systems, antisense and RNAi-mediated gene silencing is popular, whereas in bacteria RNAi mechanisms are absent and antisense technology is less developed and applied.

Expressed antisense RNAs (asRNAs) appear to be suitable for conditional gene silencing in diverse bacteria (1,2) and for large scale applications. Indeed, asRNA can repress translation in diverse bacteria (3–8), and library screens have revealed effective antisense transcripts and putative new essential genes (9,10) and inhibitors (11). The expressed asRNA method may be more efficient in Gram-positive bacteria such as *Staphylococcus aureus* (5,9–11) and *Clostridium acetobutylicum* (7,12) relative to Gram-negative bacteria, such as *Escherichia coli*, but reports of mixed results (13) suggest that design improvements are needed. Also, bacteria have endogenous asRNA regulators (14) and cell permeable modified antisense agents are efficient inhibitors (15,16). Therefore, achieving improved antisense silencing in *E.coli* appears to be largely a technical challenge.

Here we found that a simple paired-termini (PT) design stabilizes asRNA cassettes and enhances conditional gene silencing in *E.coli*. Two well-characterized and tractable genes were targeted using a range of design variants. The results show that PTasRNAs are stabilized, accumulate following induction and provide reliable gene inhibition that is sufficient to alter growth phenotypes. The approach is compatible with comprehensive forward and reverse RNA-level genetics of both essential and non-essential bacterial genes and there are potential applications in pharmaceutical discovery and metabolic engineering.

MATERIALS AND METHODS

Culture conditions and general techniques

Luria–Bertani (LB) media are comprised of 1% Bacto tryptone, 0.5% Bacto yeast extract and 0.5% NaCl. M9 media comprises 17 mg/ml Na_2HPO_4 $12H_2O$, 3 mg/ml KH_2PO_4, 0.5 mg/ml NaCl, 1 mg/ml NH_4Cl, 2 mM $MgSO_4$, 0.1 mM $CaCl_2$, 50 mg/ml leucine [TOP10 (Invitrogen Corp.) is a leucine auxotrophic strain]. *E.coli* TOP10 strain was used as a host cell throughout the experiments and grown in LB media at 37°C if not otherwise specified. M9 media with 2% glucose or with 2 mg/ml sodium acetate or M9Z media (M9 media plus 0.1% NZ-amine) with 2% glucose was used. Antibiotics were included to maintain

*To whom correspondence should be addressed. Tel: +46 8 5248 6385, Fax: +46 8 32 39 50; Email: liam.good@ki.se

plasmids at the following concentrations; chloramphenicol, 34 μg/ml; kanamycin, 20 μg/ml; ampicillin, 70 μg/ml for LB media or 35 μg/ml for M9-based media. For induction, transformants pre-grown overnight in the absence of the inducer were diluted 1:400 with the media containing one of the inducers and grown to logarithmic phase (absorbance at 550 nm = 0.6–0.8). As an inducer, 0.2% of arabinose or 1 mM of IPTG in final concentration was used if not otherwise specified. In the absence of inducer, no inhibition of target gene expression was observed in all experiments unless the constitutive promoter was used (data not shown).

Plasmid constructs and further information are described in Supplementary Materials and Methods, Figure S1 and Table S1.

Cell extracts in phosphate-buffered saline were prepared using Silica beads (0.1 mm diameter, www.biospec.com) and a Beadbeater 3110BX (www.biospec.com). Protein concentration was estimated by Bradford-assay (Bio-Rad laboratories Inc.). β-Galactosidase activity was measured as described Ref. (16). All *P*-values are two tailed and were calculated at http://faculty.vassar.edu/lowry/VassarStats.html.

Extracellular acetate concentration was measured with an enzymatic test kit (Boehringer-Mannheim, Darmstadt, Germany) according to the manufacturer's instruction.

AckA assay

Cell extracts (20 μl, typically 1 mg/ml of protein concentration) were mixed with 60 μl of reaction buffer [200 mM Tris–HCl (pH 8.0), 10 mM ATP, 267 mM potassium acetate, 10 mM $MgCl_2$, 6% hydroxylamine hydrochloride (neutralized with KOH before using)] and incubated for 60 min at 37°C (17). The reaction was stopped by the addition of 60 μl of 10% trichloroacetic acid followed by the addition of 10 μl of 2.5% $FeCl_3$ (dissolved in 2N HCl). After the debris was removed by brief centrifugation, 120 μl of the mixture was transferred to the 96-well plate (FALCON 3072, Becton Dickinson Labware Co.) and absorbance of red color was measured at 540 nm (A_1540) using VERSAmax spectrophotometer (Molecular Devices Corporation, CA, USA). As a control, the same reaction was performed with PBS substituted for cell extract (A_0540). A_0540 values were subtracted from A_1540 values ($A_1540 - A_0540 = A_2540$) and activity was calculated as A_2540/mg protein/ml (units).

Pta assay

The reaction mixture (180 μl) was prepared in the 96-well plate and contained 200 mM Tris–HCl (pH 8.0), 5 mM $MgCl_2$, 9.8 mM NAD^+, 3.75 mM CoA, 15 mM malic acid, 20 mM acetyl phosphate (lithium potassium salt), 2.3 U/μl citrate synthase, 3.3 U/μl malate dehydrogenase and cell extract (typically, 0.05 mg/ml of protein concentration) at 37°C (18). Absorbance of NADH was read at 340 nm each minute and the slope of the conversion curve was used to calculate the specific activity/mg protein/min/ml.

GFP assay

To measure green fluorescent protein (GFP) fluorescence in liquid media, transformants were cultured in a flask containing 12 ml M9Z glucose media and IPTG was added at culture density 0.6–0.7. GFP fluorescence was monitored with a NOVOstar fluorescence/luminescence reader (BMG Labtechnologies) with 180 μl cell culture placed in a 96-well plate (COSTAR 3632, Corning Inc.), using 390 nm excitation and 520 nm emission wavelengths. GFP fluorescence on solid media was detected on inverted plates using a Typhoon 9400 (Amersham Biosciences) with 488 excitation and 520 emission filters.

RNA analysis by northern blot

Total RNAs were purified by the hot acid-phenol method (19). To determine RNA half-lives, cells were treated with 250 μg/ml of rifampicin [stock solution was dissolved with dimethyl sulfoxide (DMSO), 50 mg/ml] and RNA degradation was stopped immediately by the addition of an ethanol–phenol solution (20). Northern blots were carried out using AlkPhosDirect Labelling and Detection System (Amersham Biosciences) according to the manufacturers' instructions. For detection of *ackA* asRNAs, ECF substrate (Amersham Biosciences) was used, whereas for *ackA-pta* mRNA, the chemiluminescent CDP-star substrate (Amersham Biosciences) was used. Typically, 25 μg/ml of total RNAs were loaded for each lane and ribosomal RNA bands were visualized by ethidium bromide staining followed by scanning with a Typhoon 9400 (excitation and emission wavelengths were 532 and 610 nm, respectively). Band densities were estimated with ImageJ software (http://rsb.info.nih.gov/ij/). A double-stranded DNA probe for *ackA* mRNA (probe A, 1.2 kb) was prepared by PCR using sSN17, sSN6 and pHN551 (see Supplementary Materials and Methods for details). Sequences of single-stranded oligonucleotide probes used for detection of *ackA* asRNAs were ATAGGTACTTCCATGTCGAGTAAGTTAGTACTG-GTTCTGAACTGCGGTAGTTC (probe B) and CCGCTTC-TGCGTTCTGATTTAATCTGTATCAGGCTGAAAATCT-TCTCTCATCCG (probe C).

Lengths of asRNAs are predicted from transcription start site of the P_{bad} or P_{trc} to the end of the stem–loop structre of the *rrnB* terminator. Predicted asRNA lengths are: *ackA* asRNA without PT, 454 bp; *ackA*-PT1 asRNA, 479 bp; *ackA*-PT2 asRNA, 495 bp; *ackA*-PT3 asRNA, 514 bp; *ackA*-PT4 asRNA, 476 bp; *ackA*-PT5 asRNA, 276 bp; *ackA*-PT6 asRNA, 336 bp; *ackA*-PT7 asRNA, 499 bp; *ackA*-PT7Δ asRNA, 460 bp.

Zone of inhibition assay on agar plates

Mixtures consisting of 8 ml LB-1.1% agar (autoclaved and cooled to 40°C), 0.04 mM IPTG and 50 μl of an overnight culture of cells harboring the *fabI*-PT7 asRNA plasmid or the control PT7 plasmid were solidified in petri dishes and 2.5 μl of inhibitor solution was applied to plate surfaces. The plates were incubated for 14 h, stained by adding 1.8 ml of acridine orange solution (60 μg/ml) and scanned with a Typhoon 9400 scanner (excitation and emission wavelengths were 488 and 526 nm, respectively). Inhibitors were dissolved in 10% DMSO. DMSO alone was not inhibitory and we conducted the same experiments in the absence of IPTG and confirmed there were no changes in zone sizes for the control strains (data not shown).

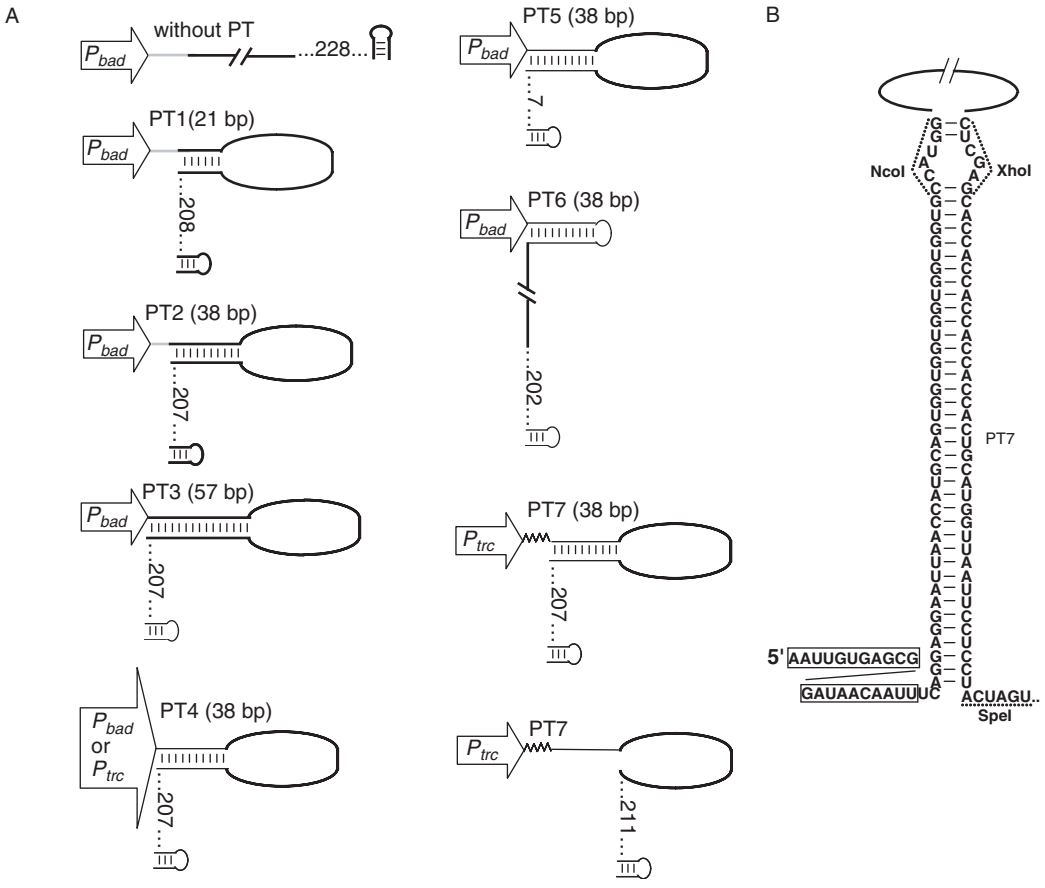

Figure 1. Expressed asRNA structures. (**A**) Thick lines (curved or linear) indicate antisense sequences (or an MCS control sequence). PT consisting of non-endogenous GC-rich sequences are indicated by thin-black lines, and thin-gray lines are 5′ leader sequences. Numbers between dots indicate the lengths of 3′ extensions (bp). All constructs end with the stem–loop structre of the *rrnB* terminator (*rrnB* T1). Arrows indicate promoters. Wavy lines indicate *lac* operator sequences. (**B**) The predicted structure of PT7-asRNA. Boxes indicate the *lac* operator.

RESULTS

asRNA expression and silencing of *ackA-lacZ*

To assess silencing by expressed RNA, we first targeted *ackA* within the *ackA-pta* operon as an example of a metabolic gene that is experimentally tractable and an interesting candidate for conditional control in industrial applications (21). AckA is central to carbon flux to and from acetate. In aerobic industrial fermentations, overflow metabolism to acetate reduces growth and inhibits macromolecule biosynthesis and product yields (22). The *ackA-pta* operon was targeted previously using standard asRNA strategies with modest effects (~10–20% inhibition) (3). To ease comparison of asRNA design parameters (Figure 1), we constructed a reporter plasmid containing *ackA-lacZ* translational fusion, where expression is driven by the native *ackA* promoter (Figure 2A). An *ackA* asRNA-expressing plasmid was constructed, containing the arabinose-inducible *bad* promoter (P_{bad}), *araC* and *rrnB* terminator. The reporter plasmid and asRNA-expressing plasmid carry different replication origins and selection markers, allowing stable maintenance of co-transformants (for details, see Supplementary Figure S1).

To benchmark our analyses to standard asRNA designs, we expressed a previously described 147 base *ackA* asRNA complementary to the 5′-untranslated region (5′-UTR) and start codon region (3), without flanking sequence modification. This construct inhibited expression only 15%, similar to the results reported earlier (3) and not significantly different than control levels ($P = 0.17$). In addition, flanking sequences that are reported to stabilize RNAs were added to the *ackA* asRNA sequence (6), including the 5′-UTR sequence of *ompA* mRNA (121 bp) (23–25), and the 3′ end of *DsrA* RNA (67 bp) (23). However, these flanking sequences did not improve inhibition (data not shown). Therefore, the existing asRNA designs did not provide sufficient silencing in these assays.

Improved gene silencing using PTasRNAs

An alternative strategy to stabilize asRNAs is to pair the termini using flanking inverted repeats to create a hairpin structure with the antisense sequence within a large loop (Figure 1). To test this design, we compared the efficacy of P_{bad}-driven *ackA* asRNA cassettes (147 bp, shown as type L in Figure 2) flanked by PT consisting of 21–57 bp. The PT contains a high GC content to strengthen pairing and resist double-stranded RNA specific RNase degradation (26) (Figure 1, PT1-3). Addition of PT to asRNA improved silencing ($P < 0.01$) and appeared to improve with PT length (Figure 2B). However, we suspect that plasmid stability is

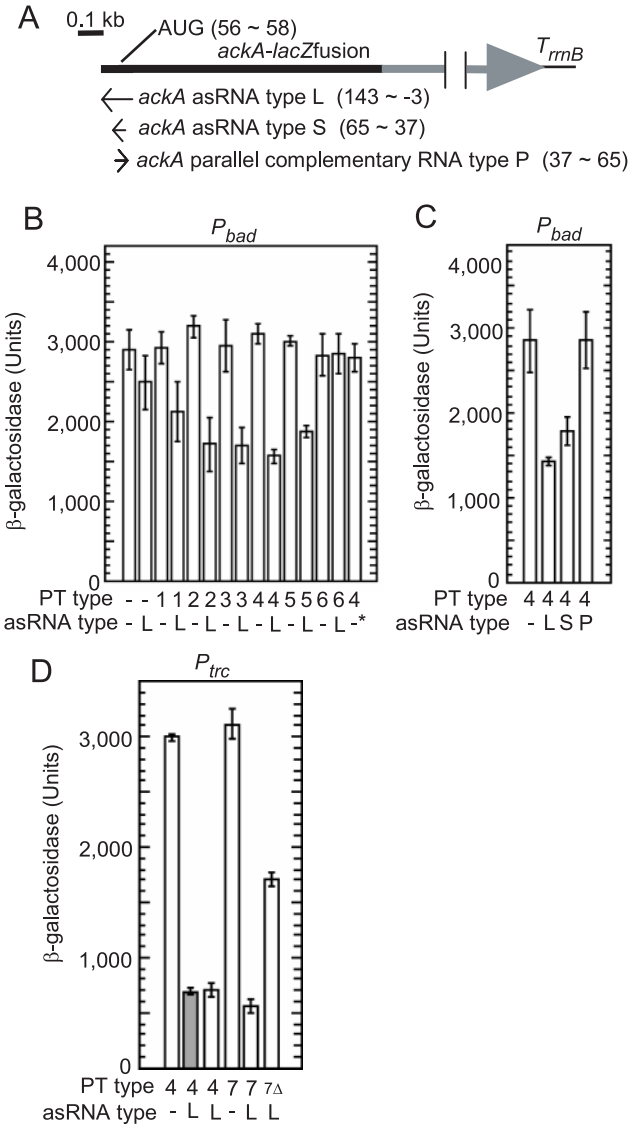

Figure 2. Silencing of plasmid-encoded *ackA-lacZ* by PT asRNAs driven by weak (P_{bad}) and strong (P_{trc}) promoters. (**A**) Schematic of the *ackA-lacZ* fusion mRNA, two types of *ackA* asRNAs (type L and type S) and an *ackA* parallel complementary RNA (type P). (**B**) Silencing by asRNAs with various PT and flanking structures. β-galactosidase activities were determined in the presence of arabinose. Cells were co-transformed with the *ackA-lacZ* reporter and *ackA* antisense plasmids. PT type (1–6, see also Figure 1) and absence (-) or presence (L) of *ackA* asRNA are shown at bottom. The '-' with an asterisk is an unrelated *bla* asRNA (191 bp) control. (**C**) Silencing by long and short asRNA cassettes as well as a parallel complementary RNA cassette. (**D**) Silencing by asRNAs driven by the P_{trc}. β-galactosidase activities are shown as in (B), except that gray and open bars indicate β-galactosidase activities in the absence and presence of IPTG, respectively. Note that PT4-asRNA driven by the P_{trc} is transcribed constitutively because the *lac* operator is absent. Average values are from triplicate experiments with std values indicated.

compromised by the longest PT, as the transformation efficiencies for PT3-containing-plasmids was lower than observed for other plasmids (data not shown) and long inverted repeats may cause plasmid loss.

To test the effects of neighboring sequences and structures, we compared several additional design variants. First, the 5′ leader sequence was removed from PT2 (PT4), and this showed no improvement ($P = 0.49$). Second, the 3′ extension extension sequence was removed from PT4 (PT5), and this even reduced inhibition ($P < 0.01$) (Figure 2B). Third, the PT structure was expressed adjacent to the antisense cassette (PT6), and this construct was not inhibitory. Also, to ensure that silencing is gene selective and dependent on an antisense sequence, we included empty vector controls and PT4-*bla* asRNA (complementary to the *bla* gene) as an unrelated control, and observed no inhibition (Figure 2B, shown in '-' and '-*'). Therefore, a 38 base PTasRNA design is advantageous over the standard design.

To assess whether antisense cassette size affects inhibition, we compared the 147 base asRNA (type L) with a shorter 29 base asRNA (type S). Both versions were inhibitory (Figure 2C), indicating that the PT design works with different sized asRNA cassettes.

As a further comparison to reported silencing technology, we expressed a 'parallel complementary RNA' designed to express a parallel sequence of the *ackA* gene; the sequence

of the *ackA* asRNA is 5′-AUCAAUUAUAGGUACUUCCA-UGUCGAGUA-3′, while the sequence of the parallel complementary RNA is 5′-AUGAGCUGUACCUUCAUGG-AUAUUAACUA-3′ (shown as type P in Figure 2A). Tchurikov and co-workers reported that the inhibition efficiency of parallel complementary RNAs exceeds asRNAs when targeted to the *lon* mRNA (8). However, we observed no inhibition with a parallel complementary RNA targeted to the *ackA* mRNA (Figure 2C). We used the 147 base asRNA for further experiments.

To further improve inhibition efficiency, the 38 base PT design (PT4) was altered by replacing P_{bad} and *araC* with P_{trc}. The P_{trc} is stronger than P_{bad} (27) and we expected the P_{trc} construct to express more asRNAs than P_{bad}. Consistent with this we observed improved inhibition (Figure 2D). This result suggests that asRNA abundance is an important parameter. To provide IPTG-inducible control to the P_{trc} construct, the *lac* operator sequence (and also $lacI^q$) was inserted (PT7) and we observed inducible *ackA* inhibition (Figure 2D). Finally, to confirm the need for PT in the PT7 construct, the downstream portion of the PT7 duplex was deleted (PT7Δ), and this construct was less effective. While less efficient than the intact PT7 construct, *ackA*-PT7Δ asRNA expressed from P_{trc} was almost as effective as *ackA*-PT4 asRNA expressed from P_{bad}. This may reflect the fact that P_{bad} is weaker than P_{trc} or that P_{bad} produces an inhomogeneous culture, containing subpopulations of differentially induced cells, due to aspects of the arabinose uptake system (28).

To test the level of genetic penetrance at the colony and cell level, another reporter plasmid containing an *ackA-DsRed* fusion (red fluorescent protein) (29) was constructed and targeted with the *ackA*-PT7 asRNA. Following *ackA*-PT7 asRNA expression, red fluorescence on plates was uniformly reduced in all colonies examined (Supplementary Figure S2) and fluorescence microscopy indicated that most cells expressed almost no red fluorescence (Supplementary Figure S2). Also, upon withdrawal of the inducer, red fluorescence was restored to control levels (Supplementary Figure S2). These results indicate that PTasRNA silencing is penetrant and reversible.

asRNA inhibition of the chromosomal *ackA-pta* operon

To test whether the effects observed with reporter constructs are observed when targeting a chromosomal gene, the effects of asRNAs with and without PT on the native *ackA-pta* expression were investigated by directly measuring AckA and Pta activities (Figure 3). Again, the best *ackA* inhibition efficiency was seen when *ackA*-PT7 asRNA was expressed from the P_{trc} (Figure 3C); 78% of AckA activity was eliminated relative to the activity of the cell expressing PT7 with no asRNA sequence. Because the *pta* gene is co-transcribed with *ackA*, Pta activity was measured following *ackA*-PT7 asRNA induction, and was reduced by 48% (Figure 3D), indicating inhibition of the whole operon. Similar downstream gene inhibition occurs when *lacZ* is inhibited within in the *lacZYA* operon (30), and this may reflect expression coordination mechanisms within operons (12).

Target and antisense RNA abundance and stability

When asRNAs hybridize with target mRNAs and inhibit gene expression, the mechanism of inhibition could be repression of translation initiation or triggered mRNA decay (5,11). To learn more about silencing by PTasRNAs, we probed *ackA-pta* mRNA abundance. Total RNAs were purified from cells grown in the presence or absence of inducers and were subjected to northern analysis (Figure 4). The asRNAs that reduced gene expression at the protein level also reduced mRNA abundance (Figure 4B, the result with probe A). The near parallel silencing pattern suggests that triggered mRNA decay is the major mechanism of antisense inhibition in this case. Residual AckA-Pta activities could be due to long half lives for these proteins following efficient mRNA silencing.

If the PTasRNAs are stabilized and expressed in large quantities, asRNA levels in cells should increase with PT addition. Therefore, we probed asRNAs in all *ackA*-asRNA

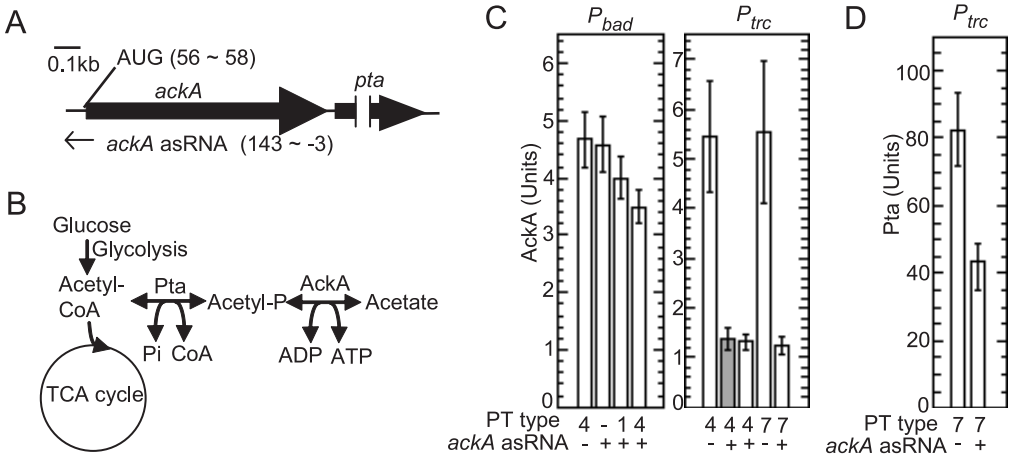

Figure 3. Inhibition of *ackA-pta* expression by asRNAs. (**A**) Schematic maps of the *ackA-pta* operon mRNA and the *ackA* asRNA are shown. (**B**) An illustration of central carbon flux. Acetyl-P is acetyl phosphate. (**C**) Silencing of AckA in the absence (a gray bar) and presence (open bars) of inducer. Cells were transformed with *ackA* antisense plasmids as indicated. Activity values are the average of three replicates with std values indicated. (**D**) Pta activity values as shown for AckA.

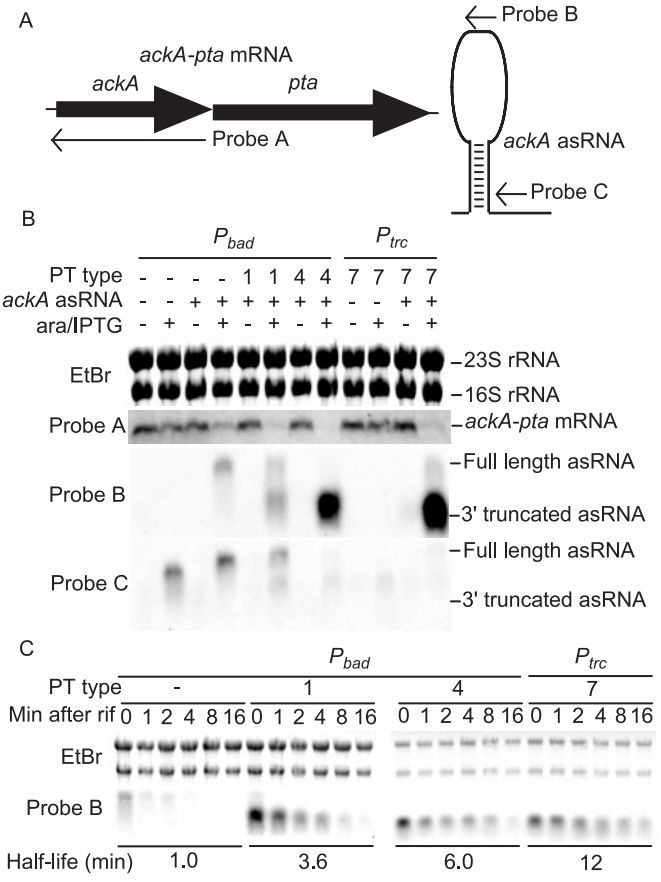

Figure 4. Northern blot analysis of *ackA* mRNA and asRNAs. (**A**) Schematic maps of the *ackA-pta* operon mRNA (left) and *ackA* asRNAs (right) with three probes (Probe A–C) used for hybridization. (**B**) Effect of PT and control structures on *ackA* mRNA and asRNA abundance. Probes A, B and C target *ackA* mRNA, the *ackA* asRNA sequence and the downstream sequence of PT, respectively. The rRNA bands stained with ethidium bromide (EtBr) were used as loading controls. (**C**) Effect of PT and control structures on asRNA half life. Total RNA was purified from cells harvested at the indicated time points following rifampicin addition and analyzed using probe B. Note that for *ackA*-PT4 and *ackA*-PT7 asRNAs the amount of total RNA loaded was only diluted 10-fold to enable quantification of the abundant asRNAs. Relative band intensities were plotted in a log–linear format and half-lives were estimated from line slopes.

expressing strains using asRNA probes B and C (Figure 4A). The probe B result (Figure 4B) shows that the amount of *ackA*-PT1 asRNA expressed from the P_{bad} was higher than *ackA* asRNA without PT (~2-fold) expressed from the P_{bad}. Also, the amounts of *ackA*-PT4 asRNA expressed from the P_{bad} and *ackA*-PT7 asRNA expressed from the P_{trc} were higher than *ackA* asRNA without PT (~15- and 24-fold, respectively). We quantified *ackA* mRNA and asRNA band intensities and confirmed a negative correlation between asRNA abundance and residual mRNA levels ($R^2 = 0.912$; $P < 0.0001$, see Supplementary Figure S3). These results further support the idea that high asRNA abundance is needed for efficient silencing.

The major bands for *ackA*-PT1 asRNA, *ackA*-PT4 asRNA and *ackA*-PT7 asRNA (lower bands, shown as 3′ truncated asRNA) migrated faster than expected. Predicted RNA lengths for *ackA* asRNA without PT, *ackA*-PT1 asRNA, *ackA*-PT4 asRNA and *ackA*-PT7 asRNA were 454, 479, 495 and 499 bp, respectively, but the major bands for PT-containing-asRNAs appeared to be ~250 bp. Furthermore, the major bands were not detected by probe C (Figure 4B, the lowest panel). These results indicate that *ackA* PTasRNAs lack 3′ end single stranded sequences, possibility due to premature termination following transcription of the PT sequences or rapid degradation of the 3′ sequences up to the paired structure. Given the lack of signals in these lanes when using probe C and the similarity between PT and Rho-independent terminators, we favor premature termination (Figure 4B, the lowest panel). Also, similar premature termination has been reported for ribozyme sequence flanked by inverted repeats (31).

Next, we determined half-lives of *ackA* asRNAs by stopping *de novo* transcription in growing cells with rifampicin. Quantification of northern band intensities (Figure 4C) showed that half-lives were prolonged by the addition of PT. Therefore, PTasRNAs are abundant and stable, and this may explain their improved efficacy. The half-life for *ackA*-PT7 asRNA expressed from the P_{trc} was twice that of *ackA*-PT4 asRNA expressed from the P_{bad}, although the PT structures differ only slightly.

To test whether the PT duplex or asRNA/mRNA duplex are cleaved by the double strand selective RNase III, the northern analyses was repeated in RNase III minus cells and in the same cells expressing plasmid-encoded RNase III. Expression of RNase III did not alter PTasRNA mobility or abundance and did not alter silencing (Supplementary Figure S4), indicating an RNase III independent silencing mechanism.

Effect of *ackA*-PTasRNAs on acetate metabolism

An *ackA-pta* deletion mutant produces less acetate than wild-type cells due to limited carbon flux to acetate (32). To test whether *ackA*-PTasRNA induction reduces acetate production, we measured acetate concentrations in liquid minimal media (M9) containing a high amount of glucose. The *ackA*-PT7 asRNA expressed from the P_{trc} was used because this construct showed the best efficiency in the earlier assays (Figure 3C). Following *ackA*-PT7 asRNA induction, acetate levels were reduced ~30% (Figure 5). Note that *E.coli* carries at least two pathways for producing acetate (AckA-Pta and PoxB pathways) (33). Therefore, acetate levels are expected to be only partially reduced with inhibition of AckA activity, as observed here.

AckA is needed for *E.coli* to use acetate as a carbon source at high acetate concentrations (acetate scavenging) (34,35). To test whether *ackA*-PT7 asRNA induction prevents growth on acetate, growth on minimal media containing either glucose or acetate as a primary carbon source was evaluated. When cells expressing the *ackA*-PT7 asRNA were grown on acetate media, colony formation was abolished completely (Figure 6). *E.coli* carries at least two pathways for scavenging acetate (AckA-Pta and Acs pathways) (33), and the present results are consistent with reports that AckA-Pta is needed for acetate scavenging (34). Essentially identical results were obtained using TOP10, wild-type K12 and BL21(DE3) (a derivative of *E.coli* B strain) strains (Figure 6), indicating that the asRNA method works well in several *E.coli* strains. Therefore, with high induction,

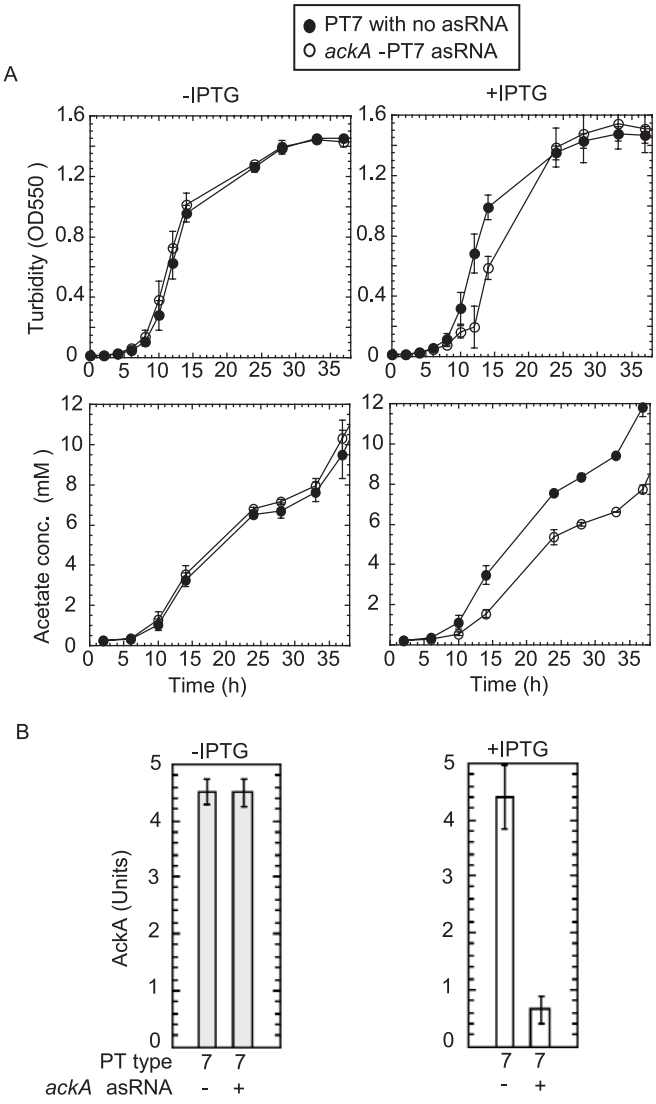

Figure 5. Effect of *ackA* asRNA on acetate production. (**A**) Culture turbidity (upper panels, absorbance at 550 nm) and extra-cellular acetate concentrations (lower panels) for each transformant are shown. Cells were grown in M9 plus glucose media with or without IPTG at 37°C. Values are the average of triplicate experiments with std values indicated. (**B**) AckA activities in cultures harvested during the logarithmic phase of growth in the absence (gray bars) and presence (open bars) of IPTG. Note that M9 plus glucose media was used in this experiment.

ackA-PT7 asRNA effects can be sufficient to mimic the phenotypes of the null mutant.

Effect of *ackA*-PTasRNAs on heterologous protein expression

Reduced acetate production is advantageous in several industrial applications. For example, *ackA-pta* negative strains show improved heterologous protein production (32), but suffer from slow growth rates. Conditional *ackA-pta* inhibition should permit rapid growth but enable carbon to be redirected from acetate at a late growth stage to enhance heterologous protein production. To test this possibility, we introduced a GFP plasmid (model of a heterologous protein) into cells containing a constitutive or inducible *ackA*-PT asRNAs plasmid. The results shown in Figure 7A indicate that final GFP fluorescence was enhanced 1.9-fold using *ackA*-PT7 and 2.5-fold using *ackA*-PT4 asRNA. Also, spot application of IPTG on cells grown on M9Z glucose plates showed increased green fluorescence when *ackA*-PT7 asRNA was co-expressed with GFP (Figure 7B).

Effect of *fabI* asRNAs on cell growth and triclosan sensitivity

To ask whether PTasRNAs are suitable for studies of genes essential for growth, we targeted the *fabI* gene encoding enoyl-ACP reductase, which is essential for fatty acid biosynthesis and vegetative growth (36) (Figure 8A). The results (Figure 8B) indicate that growth inhibition was observed only when cells harboring the *fabI*-PT7 asRNA plasmid were plated onto 1 mM IPTG-containing media. We also expressed *fabI* asRNAs lacking PT from P_{bad} and no inhibition was observed (data not shown). Again, the inhibition efficiency of PT7-asRNA expressed from P_{trc} was higher than when using the standard design, indicating that this PT design provides a reliable strategy to inhibit target gene expression.

If the growth inhibitory *fabI* asRNAs are *fabI* selective, partial inhibition should sensitize cells to the FabI inhibitor, triclosan (37,38), but not to inhibitors that target other cellular processes. To evaluate inhibitor sensitivity, we used a zone of inhibition assay (11) and *fabI* expression was partially silenced using *fabI*-PT7 asRNA induced with 0.04 mM of IPTG (Figure 8C). On plates containing cells expressing *fabI*-PT7 asRNA, the zone of clearing for triclosan was enlarged relative to cells expressing control PT7 RNA without an antisense insert, indicating sensitization. Zone sizes were not altered for the unrelated inhibitors, trimethoprim (inhibitor of dihydrofolate reductase type I) and rifampicin (inhibitor for RNA polymerase β subunit) (Figure 8C). Therefore, cells expressing *fabI*-PT7 asRNA are selectively sensitized to triclosan.

DISCUSSION

PT asRNAs provide improved gene silencing tools for *E.coli*. Bacterial RNAs are typically short lived, and there is evidence that half-life is an important factor in asRNA efficacy (2,6) and that a molar excess of asRNAs (and ribozymes) is required for efficient inhibition (4). An excess relative abundance should enable asRNAs to efficiently out-compete ribosomes at target RNAs. Therefore, the improved efficacy of PTasRNAs appears to be due to improved stability, which raises asRNA abundance. Also, it is possible that termini pairing aids target recognition by constraining the folded RNA. Finally, following mRNA recognition, PTasRNAs may trigger intrinsic decay mechanisms (39), which are apparently independent of RNase III, but may involve RNase E, or other RNases.

PTasRNAs are effective, yet we suspect that further improvements are possible. For example, target site position and length issues are not well addressed here, nor in the literature, although it is clear that target selection is an important factor. Most natural asRNAs target the translation

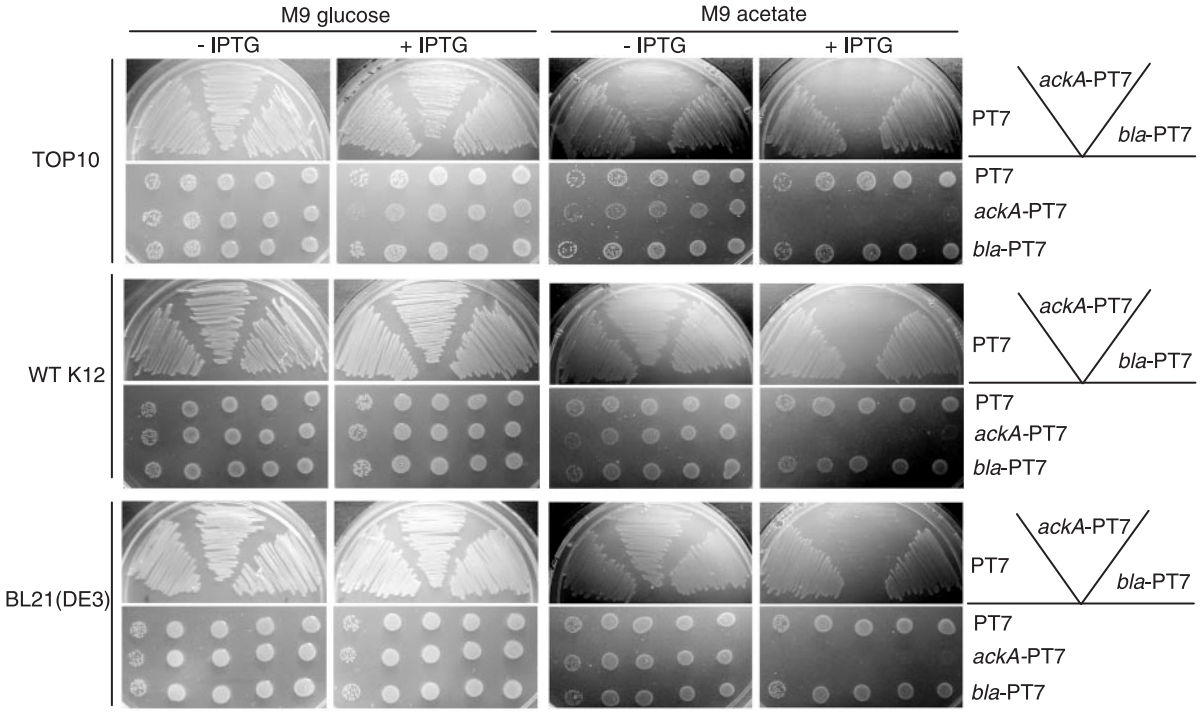

Figure 6. Effect of *ackA* PTasRNA on cell growth on glucose or acetate media. TOP10 (upper two panels), WT K12 (middle two panels) or BL21(DE3) cells (lower two panels) carrying the indicated plasmids were streaked from colonies (upper panels). Cells were spotted from liquid pre-culture serially diluted 1:10 (lower panels), where the spots at right are for 2.5 µl cultures diluted $1:10^1$ from the pre-culture and the left-most spots are for 2.5 µl aliquots diluted $1:10^5$ from pre-cultures. Cells were grown on M9 solid media with either 2% glucose or 2 mg/ml sodium acetate as a carbon source at 37°C. In the absence of IPTG, the TOP10 cells harboring *ackA*-PT7 asRNA-expressing plasmid grew slowly compared to control cells, indicating that *ackA*-PT7 asRNA expression was leaky.

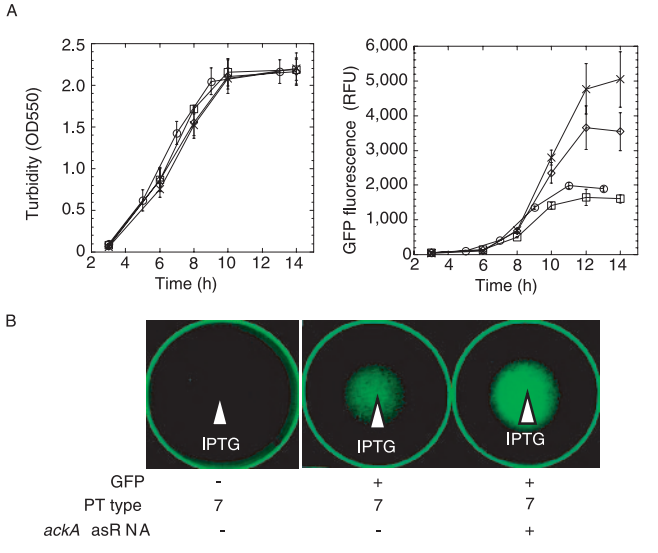

Figure 7. Expression of *ackA*-PTasRNAs enhances GFP expression. (**A**) GFP expression in M9Z glucose broth following *ackA*-asRNAs co-expression. Expressed RNAs include control PT7 with no asRNA (squares), *ackA*-PT7 asRNA (diamonds) and *ackA*-PT4 asRNA (crosses). As an additional control, cells with only the GFP expression plasmid (circles) were included. The left panel shows growth curves and the right panel shows relative GFP fluorescence intensity. Averaged values from triplicate experiments are shown with sem. Note that the PT4-asRNA is expressed constitutively. (**B**) GFP expression on solid media. The co-transformants were pre-grown overnight in liquid media, 5 µl aliquots were diluted with 200 µl of M9Z glucose media and plated evenly throughout the M9Z glucose solid media, and 5 µl of 1M IPTG was spotted onto the center of the plates. Plates were incubated for 24 h. Points of IPTG application are indicted by arrows.

initiation region (40,41), and we suspect that this region is a reasonable choice for most genes, but other susceptible regions exist (11). Successful asRNA cassettes as short as 12mer have been reported (6); however, in the absence of knowledge about target accessibility, we favor larger antisense cassettes, which are more likely to contain structures that efficiently seed hybridization. Indeed, we found that the inhibition efficiency of a 147 base cassette exceeded that of a 29 base cassette (Figure 2C). Further comparisons are needed on this issue, and target accessibility prediction tools (12,42) may be helpful. Also, *recA*$^-$ strains showed more stable inhibition (data not shown) and we observed improved results in solid media relative to liquid media, possibly due to plasmid stability problems in liquid culture. Plasmid stability is a common problem, and plasmids containing growth inhibitory sequences and long inverted repeats may be unstable (43). Therefore, PT length should be the minimum that provides asRNA stability without compromising plasmid stability. Therefore, while the PT design proved effective against all genes and in all strains tested, it is clear that plasmid stability requires attention.

The effects of PTasRNAs may reflect the action of certain natural RNAs. For example, natural asRNAs are also stabilized by paired sequences, and in the case of the FinP natural asRNA, stability and target interaction is promoted by the RNA chaperone FinO recognition of paired sequences (44). Also, the R1 plasmid encoded Hok toxin mRNA is processed into a stable isoform with perfectly matched PT (45). Therefore, PTasRNA effects may reflect endogenous mechanisms for stabilizing RNA and promoting interactions.

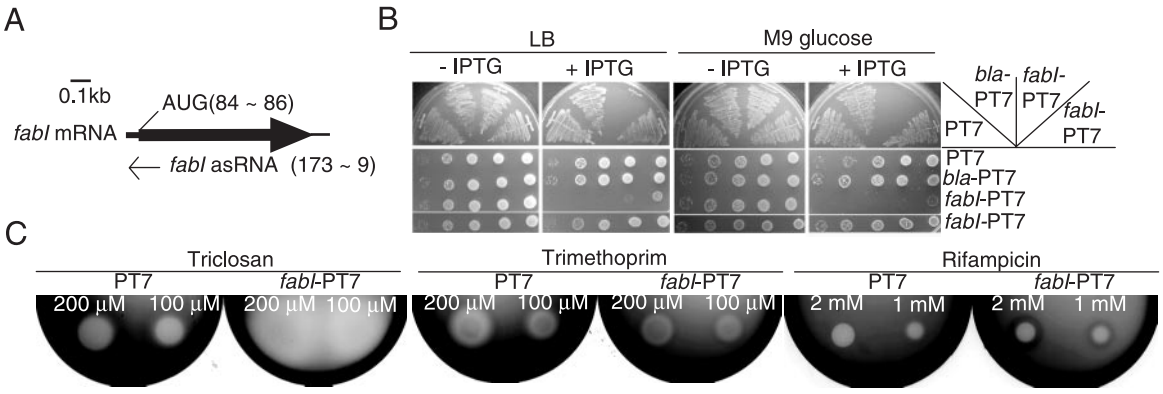

Figure 8. Effect of *fabI* asRNAs on cell growth and sensitivity to triclosan. (**A**) Schematic map of the *fabI* mRNA and the *fabI* asRNA. (**B**) Cells expressing asRNAs were streaked from plate colonies (upper panels). Expressed asRNAs were PT7 lacking asRNA (PT7, negative control), *bla*-PT7 asRNA (*bla*-PT7, unrelated control), *fabI*-PT7 asRNA (*fabI*-PT7) and *fabI*-PT7Δ asRNA (*fabI*-PT7Δ, stem deletion control). Cells were spotted as in Figure 6. (**C**) Sensitivity of asRNA expressing cells to antimicrobials. The size of the zones of inhibition indicate sensitivity. Note that growth was barely visible on the plate where triclosan was spotted onto *fabI*-PT7 asRNA-expressing-cells.

The PTasRNA design provides a framework to optimize and apply asRNA gene silencing in many applications. Forward and reverse RNA level genetics can be considered (46), and there are potential applications in pharmaceutical discovery and metabolic engineering. For example, improved conditional redirection of metabolic flux could enhance metabolic engineering, and here we show that *ackA* asRNA induction in mid-growth phase increases heterologous gene expression. Also, silencing of essential genes can aid discovery of much needed new antimicrobials (11,40), as demonstrated recently with the discovery of platensimycin (47), and here we show improved drug target silencing and inhibitor sensitization. Finally, for applications in other bacterial species, interspecies differences in asRNA and RNase activities (48,49) should be considered, but we suspect that the PT design and information about the stability and abundance of asRNAs will enable improved silencing.

SUPPLEMENTARY DATA

Supplementary Data are available at NAR online.

ACKNOWLEDGEMENTS

We thank the Swedish Research Council for support, and Sherif Abou Elela, Thomas Bentin, Henrik Nielsen, Eric Massé and our lab colleagues for comments and help. Funding to pay the Open Access publication charges for this article was provided by the Swedish Research Council.

Conflict of interest statement. None declared.

REFERENCES

1. Yin,D. and Ji,Y. (2002) Genomic analysis using conditional phenotypes generated by antisense RNA. *Curr. Opin. Microbiol*., **5**, 330–333.
2. Engdahl,H.M., Hjalt,T.A. and Wagner,E.G. (1997) A two unit antisense RNA cassette test system for silencing of target genes. *Nucleic Acids Res*., **25**, 3218–3227.
3. Kim,J.Y. and Cha,H.J. (2003) Down-regulation of acetate pathway through antisense strategy in *Escherichia coli*: improved foreign protein production. *Biotechnol. Bioeng*., **83**, 841–853.
4. Chen,H., Ferbeyre,G. and Cedergren,R. (1997) Efficient hammerhead ribozyme and antisense RNA targeting in a slow ribosome *Escherichia coli* mutant. *Nat. Biotechnol*., **15**, 432–435.
5. Ji,Y., Yin,D., Fox,B., Holmes,D.J., Payne,D. and Rosenberg,M. (2004) Validation of antibacterial mechanism of action using regulated antisense RNA expression in *Staphylococcus aureus*. *FEMS Microbiol. Lett*., **231**, 177–184.
6. Engdahl,H.M., Lindell,M. and Wagner,E.G. (2001) Introduction of an RNA stability element at the 5′ end of an antisense RNA cassette increases the inhibition of target RNA translation. *Antisense Nucleic Acid Drug Dev*., **11**, 29–40.
7. Desai,R.P. and Papoutsakis,E.T. (1999) Antisense RNA strategies for metabolic engineering of *Clostridium acetobutylicum*. *Appl. Environ. Microbiol*., **65**, 936–945.
8. Tchurikov,N.A., Chistyakova,L.G., Zavilgelsky,G.B., Manukhov,I.V., Chernov,B.K. and Golova,Y.B. (2000) Gene-specific silencing by expression of parallel complementary RNA in *Escherichia coli*. *J. Biol. Chem*., **275**, 26523–26529.
9. Ji,Y., Zhang,B., Van Horn,S.F., Warren,P., Woodnutt,G., Burnham,M.K. and Rosenberg,M. (2001) Identification of critical staphylococcal genes using conditional phenotypes generated by antisense RNA. *Science*, **293**, 2266–2269.
10. Forsyth,R.A., Haselbeck,R.J., Ohlsen,K.L., Yamamoto,R.T., Xu,H., Trawick,J.D., Wall,D., Wang,L., Brown-Driver,V., Froelich,J.M. *et al*. (2002) A genome-wide strategy for the identification of essential genes in *Staphylococcus aureus*. *Mol. Microbiol*., **43**, 1387–1400.
11. Young,K., Jayasuriya,H., Ondeyka,J.G., Herath,K., Zhang,C., Kodali,S., Galgoci,A., Painter,R., Brown-Driver,V., Yamamoto,R. *et al*. (2006) Discovery of FabH/FabF inhibitors from natural products. *Antimicrob. Agents Chemother*., **50**, 519–526.
12. Tummala,S.B., Welker,N.E. and Papoutsakis,E.T. (2003) Design of antisense RNA constructs for downregulation of the acetone formation pathway of *Clostridium acetobutylicum*. *J. Bacteriol*., **185**, 1923–1934.
13. Wagner,E.G. and Flärdh,K. (2002) Antisense RNAs everywhere? *Trends Genet*., **18**, 223–226.
14. Wagner,E.G., Altuvia,S. and Romby,P. (2002) Antisense RNAs in bacteria and their genetic elements. *Adv. Genet*., **46**, 361–398.
15. Tilley,L.D., Hine,O.S., Kellogg,J.A., Hassinger,J.N., Weller,D.D., Iversen,P.L. and Geller,B.L. (2006) Gene-specific effects of antisense phosphorodiamidate morpholino oligomer-peptide conjugates on *Escherichia coli* and *Salmonella enterica* serovar typhimurium in pure culture and in tissue culture. *Antimicrob. Agents Chemother*., **50**, 2789–2796.
16. Good,L., Awasthi,S.K., Dryselius,R., Larsson,O. and Nielsen,P.E. (2001) Bactericidal antisense effects of peptide-PNA conjugates. *Nat. Biotechnol*., **19**, 360–364.
17. Rose,I.A., Grunberg-Manago,M., Korey,S.R. and Ochoa,S. (1954) Enzymatic phosphorylation of acetate. *J. Biol. Chem*., **211**, 737–756.

18. Brown,T.D.K., Jose-Mortimer,M.C. and Kornberg,H.L. (1977) The enzymatic interconversion of acetate and acetyl-coenzyme A in *Escherichia coli*. *J. Gen. Microbiol.*, **102**, 327–336.
19. Aiba,H., Adhya,S. and de Crombrugghe,B. (1981) Evidence for two functional gal promoters in intact *Escherichia coli* cells. *J. Biol. Chem.*, **256**, 11905–11910.
20. Thanbichler,M. and Böck,A. (2002) The function of SECIS RNA in translational control of gene expression in *Escherichia coli*. *EMBO J.*, **21**, 6925–6934.
21. Yang,Y.T., Aristidou,A.A., San,K.Y. and Bennett,G.N. (1999) Metabolic flux analysis of *Escherichia coli* deficient in the acetate production pathway and expressing the *Bacillus subtilis* acetolactate synthase. *Metab. Eng.*, **1**, 26–34.
22. Cho,S., Shin,D., Ji,G.E., Heu,S. and Ryu,S. (2005) High-level recombinant protein production by overexpression of Mlc in *Escherichia coli*. *J. Biotechnol.*, **119**, 197–203.
23. Moll,I., Afonyushkin,T., Vytvytska,O., Kaberdin,V.R. and Bläsi,U. (2003) Coincident Hfq binding and RNase E cleavage sites on mRNA and small regulatory RNAs. *RNA*, **9**, 1308–1314.
24. Rasmussen,A.A., Eriksen,M., Gilany,K., Udesen,C., Franch,T., Petersen,C. and Valentin-Hansen,P. (2005) Regulation of *ompA* mRNA stability: the role of a small regulatory RNA in growth phase-dependent control. *Mol. Microbiol.*, **58**, 1421–1429.
25. Arnold,T.E., Yu,J. and Belasco,J.G. (1998) mRNA stabilization by the *ompA* 5′-untranslated region: two protective elements hinder distinct pathways for mRNA degradation. *RNA*, **4**, 319–330.
26. Lamontagne,B. and Elela,S.A. (2004) Evaluation of the RNA determinants for bacterial and yeast RNase III binding and cleavage. *J. Biol. Chem.*, **279**, 2231–2241.
27. Baneyx,F. (1999) Recombinant protein expression in *Escherichia coli*. *Curr. Opin. Biotechnol.*, **10**, 411–421.
28. Khlebnikov,A. and Keasling,J.D. (2002) Effect of *lacY* expression on homogeneity of induction from the P_{tac} and P_{trc} promoters by natural and synthetic inducers. *Biotechnol. Prog.*, **18**, 672–674.
29. Bevis,B.J. and Glick,B.S. (2002) Rapidly maturing variants of the Discosoma red fluorescent protein (DsRed). *Nat. Biotechnol.*, **20**, 83–87.
30. Pestka,S., Daugherty,B.L., Jung,V., Hotta,K. and Pestka,R.K. (1984) Anti-mRNA: specific inhibition of translation of single mRNA molecules. *Proc. Natl Acad. Sci. USA*, **81**, 7525–7528.
31. Deshler,J.O., Li,H., Rossi,J.J. and Castanotto,D. (1995) Ribozymes expressed within the loop of a natural antisense RNA form functional transcription terminators. *Gene*, **155**, 35–43.
32. Bauer,K.A., Ben-Bassat,A., Dawson,M., de la Puente,V.T. and Neway,J.O. (1990) Improved expression of human interleukin-2 in high-cell-density fermentor cultures of *Escherichia coli* K-12 by a phosphotransacetylase mutant. *Appl. Environ. Microbiol.*, **56**, 1296–1302.
33. Phue,J.N., Noronha,S.B., Hattacharyya,R., Wolfe,A.J. and Shiloach,J. (2005) Glucose metabolism at high density growth of *E.coli* B and *E.coli* K: differences in metabolic pathways are responsible for efficient glucose utilization in *E.coli* B as determined by microarrays and northern blot analyses. *Biotechnol. Bioeng.*, **90**, 805–820.
34. Wolfe,A.J. (2005) The acetate switch. *Microbiol. Mol. Biol. Rev.*, **69**, 12–50.
35. LeVine,S.M., Ardeshir,F. and Ames,G.F. (1980) Isolation and characterization of acetate kinase and phosphotransacetylase mutants of *Escherichia coli* and *Salmonella typhimurium*. *J. Bacteriol.*, **143**, 1081–1085.
36. Bergler,H., Fuchsbichler,S., Högenauer,G. and Turnowsky,F. (1996) The enoyl-[acyl-carrier-protein] reductase (FabI) of *Escherichia coli*, which catalyzes a key regulatory step in fatty acid biosynthesis, accepts NADH and NADPH as cofactors and is inhibited by palmitoyl-CoA. *Eur. J. Biochem.*, **242**, 689–694.
37. Dryselius,R., Aswasti,S.K., Rajarao,G.K., Nielsen,P.E. and Good,L. (2003) The translation start codon region is sensitive to antisense PNA inhibition in *Escherichia coli*. *Oligonucleotides*, **13**, 427–433.
38. DeVito,J.A., Mills,J.A., Liu,V.G., Agarwal,A., Sizemore,C.F., Yao,Z., Stoughton,D.M., Cappiello,M.G., Barbosa,M.D., Foster,L.A. *et al.* (2002) An array of target-specific screening strains for antibacterial discovery. *Nat. Biotechnol.*, **20**, 478–483.
39. Massé,E., Escorcia,F.E. and Gottesman,S. (2003) Coupled degradation of a small regulatory RNA and its mRNA targets in *Escherichia coli*. *Genes Dev.*, **17**, 2374–2383.
40. Dryselius,R., Nekhotiaeva,N. and Good,L. (2005) Antimicrobial synergy between mRNA- and protein-level inhibitors. *J. Antimicrob. Chemother.*, **56**, 97–103.
41. Good,L. (2003) Translation repression by antisense sequences. *Cell. Mol. Life Sci.*, **60**, 854–861.
42. Ding,Y., Chan,C.Y. and Lawrence,C.E. (2004) Sfold web server for statistical folding and rational design of nucleic acids. *Nucleic Acids Res.*, **32**, W135–W141.
43. Shafferman,A., Flashner,Y., Hertman,I., Olami,Y. and Cohen,S. (1987) Molecular aspects of genetic instability of an artificial 68 bp perfect palindrome in *Escherichia coli*. *Mol. Gen. Genet.*, **208**, 294–300.
44. Arthur,D.C., Ghetu,A.F., Gubbins,M.J., Edwards,R.A., Frost,L.S. and Glover,J.N. (2003) FinO is an RNA chaperone that facilitates sense-antisense RNA interactions. *EMBO J.*, **22**, 6346–6355.
45. Franch,T., Gultyaev,A.P. and Gerdes,K. (1997) Programmed cell death by *hok*/*sok* of plasmid R1: processing at the *hok* mRNA 3′ end triggers structural rearrangements that allow translation and antisense RNA binding. *J. Mol. Biol.*, **273**, 38–51.
46. Moffat,J. and Sabatini,D.M. (2006) Building mammalian signalling pathways with RNAi screens. *Nature Rev. Mol. Cell Biol.*, **7**, 177–187.
47. Wang,J., Soisson,S.M., Young,K., Shoop,W., Kodali,S., Galgoci,A., Painter,R., Parthasarathy,G., Tang,Y.S., Cummings,R. *et al.* (2006) Platensimycin is a selective FabF inhibitor with potent antibiotic properties. *Nature*, **441**, 358–361.
48. Brantl,S. and Wagner,E.G. (2002) An antisense RNA-mediated transcriptional attenuation mechanism functions in *Escherichia coli*. *J. Bacteriol.*, **184**, 2740–2747.
49. Condon,C. (2003) RNA processing and degradation in *Bacillus subtilis*. *Microbiol. Mol. Biol. Rev.*, **67**, 157–174.